

Interplay between pairing and correlations in spin-polarized bound states

S. Głodzik,¹ A. Kobiałka,¹ A. Gorczyca-Goraj,² A. Ptok,³ G. Górski,⁴ M. M. Maška,² and T. Domański^{1,*}

¹*Institute of Physics, M. Curie-Skłodowska University, 20-031 Lublin, Poland*

²*Institute of Physics, University of Silesia, 41-500 Chorzów, Poland*

³*Institute of Nuclear Physics, Polish Academy of Sciences, 31-342 Kraków, Poland*

⁴*Faculty of Mathematics and Natural Sciences, University of Rzeszów, 35-310 Rzeszów, Poland*

(Dated: April 6, 2024)

We investigate the single and multiple defects embedded in a superconducting host, studying interplay between the proximity induced pairing and interactions. We explore influence of the spin-orbit coupling on energies, polarization and spatial patterns of the bound (Yu-Shiba-Rusinov) states of magnetic impurities in 2-dimensional square lattice. We also address the peculiar bound states in the proximitized Rashba chain, resembling the Majorana quasiparticles, focusing on their magnetic polarization which has been recently reported by [S. Jeon *et al.*, *Science* **358**, 772 (2017)]. Finally, we study leakage of these polarized Majorana quasiparticles on the side-attached nanoscopic regions and confront them with the subgap Kondo effect near to the singlet-doublet phase transition.

I. INTRODUCTION

Magnetism is usually detrimental to superconductivity because it breaks the Cooper pairs (at critical H_{c2}). There are, however, a few exceptions when these phenomena coexist e.g. in iron pnictides [1], CeCoIn₅ [2] or sometimes magnetic field induces superconductivity [3]. Plenty of other interesting examples can be found in nanoscopic systems, where magnetic impurities (dots) have more subtle relationship with the electron pairing driven by the proximity effect [4, 5]. Cooper pairs easily penetrate the nanoscopic impurities, inducing the bound (Yu-Shiba-Rusinov) states that manifest the local pairing coexisting with magnetic polarization. Such bound states have been observed in various systems [6–14]. In-gap states (appearing in pairs symmetrically around the Fermi level) can be nowadays controlled electrostatically or magnetically [12] whereas their topography, spatial extent and polarization can be precisely inspected by the state-of-art tunneling measurements [15, 16].

It has been reported that adatoms deposited on 2-dimensional superconducting surface develop the Yu-Shiba-Rusinov (YSR) states, extending to a dozen of intersite distances and they reveal the particle-hole oscillations [11]. Bound states of these magnetic impurities in a superconducting NbSe₂ are characterized by the star shape [17] typical for the rotational symmetry of its triangular lattice. More complex objects (like dimers) reveal other spatial features, showing the bonding and antibonding states [18]. In a somewhat different context it has been pointed out [19] that exchange coupling between numerous quantum defects involving their intrinsic spins can couple them ferromagnetically, and this can be used (e.g. in metallic carbon nanotubes) for a robust transmission of magnetic information at large distances.

In all cases the bound YSR states are also sensitive to interactions. One of them is the spin-orbit coupling

(usually meaningful at boundaries, e.g. surfaces) [20–22]. Such interaction in one-dimensional magnetic nanowires can induce the topologically nontrivial superconducting phase, in which the YSR states undergo mutation to the Majorana (zero-energy) quasiparticles. Coulomb repulsion between the opposite spin electrons can bring additional important effects. In the proximitized quantum dots it can lead to a parity change (quantum phase transition) with further influence on the subgap Kondo effect (driven by effective spin-exchange coupling with mobile electrons). Furthermore, such spin exchange can be amplified by the induced electron pairing, and can have constructive influence on the Kondo effect [23, 24].

We study here the polarized bound states, taking into account the spin-orbit and/or Coulomb interactions. In particular, we consider: (i) the single magnetic impurity in 2-dimensional square lattice of a superconducting host, (ii) nanoscopic chain of the magnetic impurities on the classical superconductor (i.e. proximitized Rashba nanowire) in its topologically trivial/nontrivial superconducting phase, and (iii) the strongly correlated quantum dot side-attached to the Rashba chain, where the Kondo and the leaking Majorana quasiparticle can be confronted with each other. These magnetically polarized YSR and Majorana quasiparticles as well as the subgap Kondo effect can be experimentally verified using the tunneling heterostructures with ferromagnetic lead (STM tip).

II. SINGLE MAGNETIC IMPURITY

Let us start by considering a single magnetic impurity on surface of the *s*-wave superconductor in presence of the spin-orbit interactions. This situation can be modelled by the Anderson-type Hamiltonian

$$\hat{\mathcal{H}} = \hat{\mathcal{H}}_{\text{sc}} + \hat{\mathcal{H}}_{\text{imp}} + \hat{\mathcal{H}}_{\text{SOC}}. \quad (1)$$

We describe the superconducting substrate by

$$\hat{\mathcal{H}}_{\text{sc}} = -t \sum_{\langle i,j \rangle \sigma} \hat{c}_{i\sigma}^\dagger \hat{c}_{j\sigma} + U \sum_i \hat{n}_{i\uparrow} \hat{n}_{i\downarrow} - \mu \sum_{i\sigma} \hat{n}_{i\sigma}, \quad (2)$$

* e-mail: doman@kft.umcs.lublin.pl

where $\hat{c}_{i\sigma}^\dagger$ ($\hat{c}_{i\sigma}$) denotes creation (annihilation) of electron with spin σ at i -th site, t is a hopping integral between the nearest-neighbors, μ is the chemical potential, and $\hat{n}_{i\sigma} = \hat{c}_{i\sigma}^\dagger \hat{c}_{i\sigma}$ is the number operator. For simplicity, we assume a weak attractive potential $U < 0$ between itinerant electrons and treat it within the mean-field decoupling $\hat{c}_{i\uparrow}^\dagger \hat{c}_{i\uparrow} \hat{c}_{i\downarrow}^\dagger \hat{c}_{i\downarrow} \approx \chi_i \hat{c}_{i\uparrow}^\dagger \hat{c}_{i\downarrow}^\dagger + \chi_i^* \hat{c}_{i\downarrow} \hat{c}_{i\uparrow} - |\chi_i|^2 + n_{i\uparrow} \hat{c}_{i\downarrow}^\dagger \hat{c}_{i\downarrow} + n_{i\downarrow} \hat{c}_{i\uparrow}^\dagger \hat{c}_{i\uparrow} - n_{i\uparrow} n_{i\downarrow}$, where $\chi_i = \langle \hat{c}_{i\downarrow} \hat{c}_{i\uparrow} \rangle$ is the local superconducting order parameter and $n_{i\sigma} = \langle \hat{n}_{i\sigma} \rangle$. The Hartree term can be incorporated into the local (spin-dependent) chemical potential $\mu \rightarrow \tilde{\mu}_{i\sigma} \equiv \mu - U n_{i\sigma}$. The second term in Eq. (1) refers to the local impurity

$$\hat{H}_{\text{imp}} = -J \left(\hat{c}_{0\uparrow}^\dagger \hat{c}_{0\uparrow} - \hat{c}_{0\downarrow}^\dagger \hat{c}_{0\downarrow} \right) + K \left(\hat{c}_{0\uparrow}^\dagger \hat{c}_{0\uparrow} + \hat{c}_{0\downarrow}^\dagger \hat{c}_{0\downarrow} \right) \quad (3)$$

which affects the order parameter χ_i near the impurity site $i=0$, inducing the YSR states [25, 26]. In this work we focus on the magnetic term J [4, 27], disregarding the potential scattering K .

The spin-orbit coupling (SOC) can be expressed by

$$\hat{H}_{\text{SOC}} = -i\lambda \sum_{ij\sigma\sigma'} \hat{c}_{i+\mathbf{d}_j\sigma}^\dagger \left(\mathbf{d}_j \times \hat{\boldsymbol{\sigma}}^{\sigma\sigma'} \right) \cdot \hat{\mathbf{w}} \hat{c}_{i\sigma'}, \quad (4)$$

where vector $\mathbf{d}_j = (d_j^x, d_j^y, 0)$ refers to positions of the nearest neighbors of i -th site, and $\hat{\boldsymbol{\sigma}} = (\sigma_x, \sigma_y, \sigma_z)$ stand for the Pauli matrices. The unit vector $\hat{\mathbf{w}}$ shows a direction of the spin orbit field, which can be arbitrary. Here we restrict our considerations to the in-plane $\hat{\mathbf{w}} \equiv \hat{x} = (1, 0, 0)$ polarization (that would be important for nontrivial superconductivity in nanowires discussed in Sec. III). The other (out-of-plane) component could eventually mix \uparrow and \downarrow spins [22].

A. Bogoliubov–de Gennes technique

Impurities break the translational invariance, therefore the pairing amplitude χ_i and occupancy $n_{i\sigma}$ have to be determined for each lattice site individually. We can diagonalize the Hamiltonian (1) by the unitary transformation

$$\hat{c}_{i\sigma} = \sum_n \left(u_{in\sigma} \hat{\gamma}_n - \sigma v_{in\sigma}^* \hat{\gamma}_n^\dagger \right), \quad (5)$$

where $\hat{\gamma}_n^{(\dagger)}$ are quasiparticle fermionic operators, with eigenvectors $u_{in\sigma}$ and $v_{in\sigma}$. This leads to the Bogoliubov–de Gennes (BdG) equations

$$\begin{pmatrix} u_{in\uparrow} \\ v_{in\downarrow} \\ u_{in\downarrow} \\ v_{in\uparrow} \end{pmatrix} \quad (6)$$

$$= \sum_j \begin{pmatrix} H_{ij\uparrow} & D_{ij} & S_{ij}^{\uparrow\downarrow} & 0 \\ D_{ij}^* & -H_{ij\downarrow}^* & 0 & S_{ij}^{\downarrow\uparrow} \\ S_{ij}^{\downarrow\uparrow} & 0 & H_{ij\downarrow} & D_{ij} \\ 0 & S_{ij}^{\uparrow\downarrow} & D_{ij}^* & -H_{ij\uparrow}^* \end{pmatrix} \begin{pmatrix} u_{jn\uparrow} \\ v_{jn\downarrow} \\ u_{jn\downarrow} \\ v_{jn\uparrow} \end{pmatrix},$$

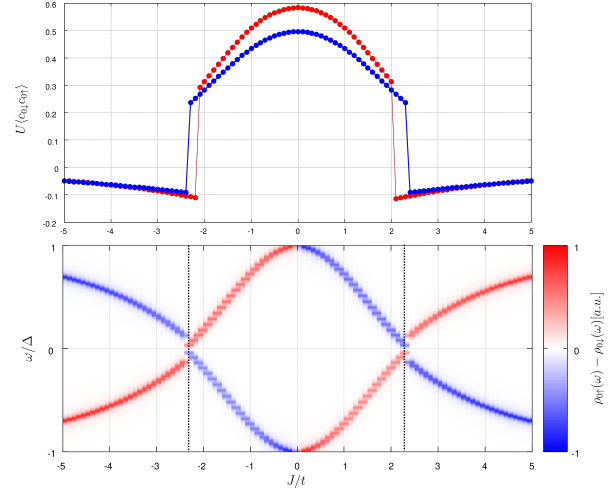


FIG. 1. The local order parameter obtained at zero temperature for the weak $\lambda/t = 0.1$ (red line) and strong spin orbit coupling $\lambda/t = 1$ (blue line). The bottom panel shows the energies and magnetic polarization $\rho_{0\uparrow}(\omega) - \rho_{0\downarrow}(\omega)$ of YSR states obtained in the weak coupling limit $\lambda/t = 0.1$.

where $D_{ij} = \delta_{ij} U \chi_i$ and the single-particle term is given by $H_{ij\sigma} = -t \delta_{\langle i,j \rangle} - (\tilde{\mu}_{i\sigma} - \sigma J \delta_{i0}) \delta_{ij} + S_{ij}^{\sigma\sigma}$ with the spin-orbit coupling term $S_{ij}^{\sigma\sigma'} = -i\lambda \sum_l \left(\mathbf{d}_l \times \hat{\boldsymbol{\sigma}}^{\sigma\sigma'} \right) \cdot \hat{\mathbf{w}} \delta_{j,i+\mathbf{d}_l}$. Here, $S_{ij}^{\sigma\sigma}$ and $S_{ij}^{\sigma\bar{\sigma}}$ (where $\bar{\sigma}$ is opposite to σ) correspond to in-plane and out-of-plane spin orbit field, respectively, which satisfy $S_{ji}^{\sigma'\sigma} = (S_{ij}^{\sigma\sigma'})^*$.

Solving numerically the BdG equations (6) we can determine the local order parameter χ_i and occupancy $n_{i\sigma}$

$$\chi_i = \sum_n \left[u_{in\downarrow} v_{in\uparrow}^* f(\mathcal{E}_n) - u_{in\uparrow} v_{in\downarrow}^* f(-\mathcal{E}_n) \right], \quad (7)$$

$$n_{i\sigma} = \sum_n \left[|u_{in\sigma}|^2 f(\mathcal{E}_n) + |v_{in\sigma}|^2 f(-\mathcal{E}_n) \right], \quad (8)$$

where $f(\omega) = [1 + \exp(\omega/k_B T)]^{-1}$. In what follows, we shall inspect the spin-resolved local density of states

$$\rho_{i\sigma}(\omega) = \sum_n \left[|u_{in\sigma}|^2 \delta(\omega - \mathcal{E}_n) + |v_{in\sigma}|^2 \delta(\omega + \mathcal{E}_n) \right].$$

For its numerical computation we replace the Dirac delta function by Lorentzian $\delta(\omega) = \zeta / [\pi(\omega^2 + \zeta^2)]$ with a small broadening $\zeta = 0.025t$. We have solved the BdG equations, considering the single magnetic impurity in a square lattice, comprising $N_a \times N_b = 41 \times 41$ sites. We assumed $U/t = -3$, $\mu/t = 0$, and determined the bound states for two representative values of the spin-orbit coupling λ upon varying J .

B. Topography of the bound states

The magnetic potential has substantial influence on the local order parameter χ_0 . In particular, at some critical value J_c this quantity discontinuously changes

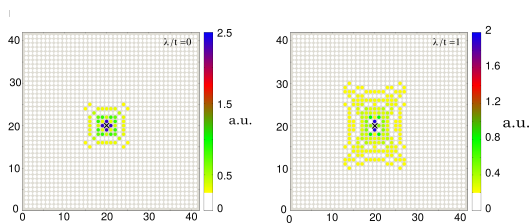


FIG. 2. Spatial profiles of the YSR states $\sum_{\sigma} \rho_{i\sigma}^+$ obtained for $|J| < J_c$ in absence of the spin-orbit coupling (left panel) and for the strong in-plane coupling $\lambda = t$ (right panel). The spin-orbit field is chosen along x axis and leads to additional imaginary hopping term along y axis, which elongates the YSR states in y direction. The impurity spin is oriented along $(0, 0, 1)$ direction.

its magnitude and sign (see the upper panel in Fig. 1), signalling the first-order phase transition [28–30]. This quantum phase transition at J_c is an artifact of the classical spin approximation. When spin fluctuations are allowed, a Kondo-like crossover is obtained instead of a first-order phase transition [31, 32]. In general, the quasiparticle spectrum at the impurity site is characterized by two bound states $\pm E_{\text{YSR}}$ inside the gap Δ of superconducting host (displayed in bottom panel of Fig. 1). These energies $\pm E_{\text{YSR}}$ and the related spectral weights depend on J . At $J = J_c$ the YSR bound states cross each other $E_{\text{YSR}}(J_c) = 0$ and their crossing signifies the ground state parity change [33] from the BCS-type (spinless) to the singly occupied (spinful) configurations [8, 15, 21, 34]. Let us remark that this quantum phase transition is also accompanied with reversal of the YSR polarization (see bottom panel in Fig. 1). Similar behavior can be observed also for the multiple impurities, at several critical values of J [35].

Within the BdG approach we can inspect spatial profiles of the YSR states by integrating the spectral weights $\rho_{i\sigma}^{\pm} = \int_{\omega_1}^{\omega_2} \rho_{i\sigma}(\omega) d\omega$ in the interval $\omega \in (\omega_1, \omega_2)$ capturing the quasiparticles at negative/positive energies $\pm E_{\text{YSR}}$ [36]. Fig. 2 illustrates the results obtained for $\lambda = 0$ (left panel) and $\lambda = t$ (right panel). We clearly notice a fourfold rotational symmetry (typical for the square lattice) and the spatial extent of YSR states reaching several sites away from the magnetic impurity. Nonvanishing difference of the spectral weights $|u_{in\uparrow}|^2 - |u_{in\downarrow}|^2$ at the positive energy $\omega = +E_{\text{YSR}}$ and $|v_{in\uparrow}|^2 - |v_{in\downarrow}|^2$ at the negative energy $\omega = -E_{\text{YSR}}$ implies effective spin-polarization of the bound states (their polarization is illustrated in the bottom panel of Fig. 1).

For some quantitative estimation of the spatially varying magnetization (driven by the particle-hole asymmetry) we have computed the *displaced moving average* $\bar{\rho}^{\pm}(r)$, corresponding to an averaged spectral weight contained in a ring of the radius r and a small half-width δr . This quantity is sensitive only to radial distance r from the magnetic impurity, averaging the angular anisotropy. Our results, presented in Fig. 3, clearly indicate the spatial particle-hole oscillations $\bar{\rho}^{\pm}(r)$ of the YSR states

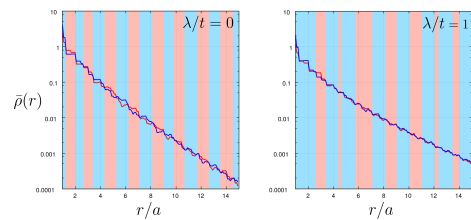


FIG. 3. Hole- (blue line) and electron-like (red line) displaced moving average $\bar{\rho}^{\pm}(r)$ as a function of radial distance r from the impurity site obtained for $|J| < J_c$ using $\delta r = 0.5a$. The (blue/red) background color indicates the dominant hole/particle type of YSR state at a given distance r . The upper and lower panels correspond to $\lambda = 0$ and $\lambda = t$, respectively.

(compare the blue and red lines). Such particle-hole oscillations decay exponentially with r in agreement with previous studies [11, 37, 38]. The dominant (particle or hole) contributions to the YSR bound states are displayed by an alternating color of the background in Fig. 3. We notice that the spin-orbit coupling seems to suppress these particle-hole oscillations.

Summarizing this section, we point out that the quantum phase transition (at J_c) depends on the spin-orbit coupling λ and it has experimentally observable consequences in the magnetization induced near the impurity site. For weak magnetic scattering $|J| < J_c$ the impurity is partly screened, whereas for the stronger couplings $|J| > J_c$ the impurity polarizes its neighborhood in a direction of its own magnetic moment. Similar effects have been previously discussed by V. Kaladzhyan *et al.* [21] but here we additionally present the role of spin orbit coupling. First of all, such interaction shifts the quantum phase transition (to larger values of J) and secondly it enhances the spatial extent of YSR states and gradually smoothens their particle-hole oscillations.

III. MAGNETICALLY POLARIZED MAJORANA QUASIPARTICLES

In this section we increase the number of impurities. Let us now imagine the nanoscopic chain of magnetic impurities (for instance Fe atoms) deposited on a surface of the conventional s -wave superconductor. We shall study the magnetically polarized bound states, focusing on the proximity induced nontrivial superconducting phase. In practice, the quasiparticle spectrum can be probed within STM-type setup, by attaching the conducting [39, 40], superconducting [41], or the magnetically polarized tip [42]. We shall assume the spin-orbit interaction perpendicularly aligned to the wire and magnetic field parallel to it, leading to the effective intersite pairing of identical spins and (under specific condition) inducing the zero-energy end modes resembling the Majorana quasiparticles. This issue has been recently studied very intensively but here we simply focus on the spin-

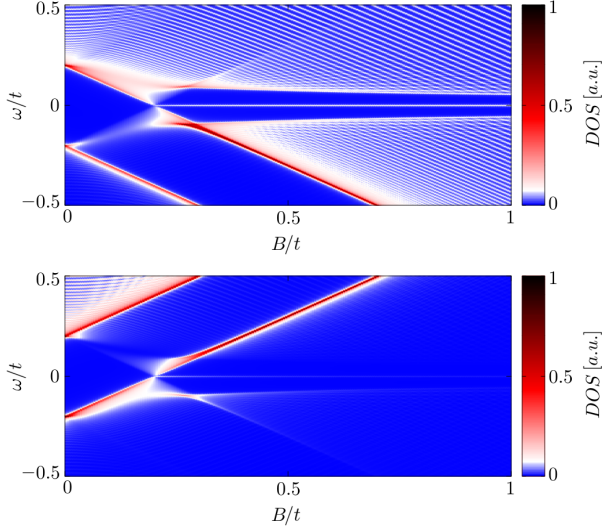


FIG. 4. The effective quasiparticle spectrum $\rho_{i,\sigma}(\omega)$ with respect to the magnetic field B aligned along the nanochain obtained for $\sigma = \uparrow$ (upper panel) and $\sigma = \downarrow$ (bottom panel). Magnetic field B is expressed in units of $t/(g\mu_B/2)$.

polarized aspects of this problem.

Due to the spin-orbit interaction, momentum and spin are no longer “good” quantum numbers. By solving the problem numerically, however, we can estimate percentage with which the true quasiparticles are represented by the initial spin. We have recently emphasized [43], that amplitude of the intersite pairing (between identical spin electrons) differs several times for \uparrow and \downarrow sectors. This leads to an obvious polarization of the YSR and Majorana quasiparticles (the latter appearing near the nanochain edges).

A. Proximitized Rashba chain

Let us consider the STM-type geometry, relevant to the recent experimental situation addressed by A. Yazdani and coworkers [42], which can be described by the following Hamiltonian

$$\hat{\mathcal{H}} = \hat{\mathcal{H}}_{\text{tip}} + \hat{\mathcal{H}}_{\text{chain}}^{\text{prox}} + \hat{\mathcal{H}}_{\text{tip-chain}}. \quad (9)$$

We assume here, that STM tip describes the polarized fermion gas $\hat{\mathcal{H}}_N = \sum_{\mathbf{k},\sigma} \xi_{\mathbf{k}N}^{\sigma} \hat{c}_{\mathbf{k}N}^{\dagger} \hat{c}_{\mathbf{k}\sigma N}$, where energy $\xi_{\mathbf{k}N}^{\sigma} = \varepsilon_{\mathbf{k}} - \mu_{N\sigma}$ can be controlled by some finite detuning of the chemical potentials $\mu_{N\uparrow} - \mu_{N\downarrow}$. Individual atoms of the nanochain are coupled with such STM tip via $\hat{\mathcal{H}}_{\text{tip-chain}} = \sum_{\mathbf{k},\sigma} \left(V_{i,\mathbf{k}N} \hat{d}_{i,\sigma}^{\dagger} \hat{c}_{\mathbf{k}\sigma N} + V_{i,\mathbf{k}\beta}^* \hat{c}_{\mathbf{k}\sigma N}^{\dagger} \hat{d}_{i,\sigma} \right)$. For simplicity, we assume constant couplings $\Gamma_{\beta} = 2\pi \sum_{\mathbf{k}} |V_{i,\mathbf{k}\beta}|^2 \delta(\omega - \xi_{\mathbf{k}\beta})$.

Low-energy physics of such proximitized Rashba

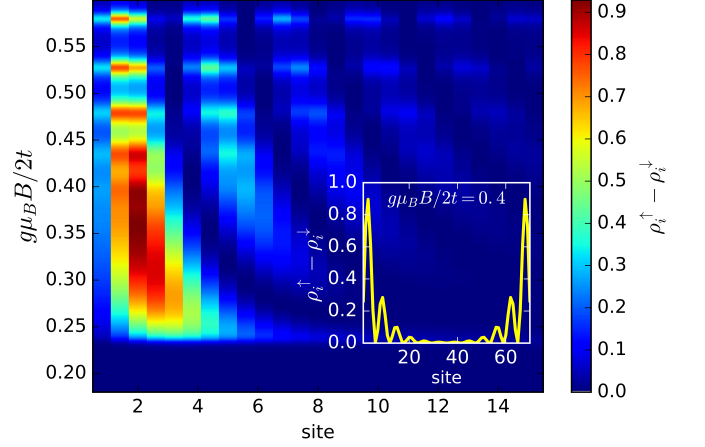


FIG. 5. Magnetically polarized spectrum $\rho_{i,\uparrow}(\omega) - \rho_{i,\downarrow}(\omega)$ at $\omega = 0$ obtained at peripheral sites of the Rashba chain.

nanowire can be described by [44]

$$\begin{aligned} \hat{\mathcal{H}}_{\text{chain}}^{\text{prox}} = & \sum_{i,j,\sigma} (t_{ij} - \delta_{ij}\mu) \hat{d}_{i,\sigma}^{\dagger} \hat{d}_{j,\sigma} + \hat{\mathcal{H}}_{\text{Rashba}} \\ & + \hat{\mathcal{H}}_{\text{Zeeman}} + \hat{\mathcal{H}}_{\text{prox}}, \end{aligned} \quad (10)$$

where $\hat{d}_{i,\sigma}^{(\dagger)}$ annihilates (creates) electron of spin σ at site i with energy ε_i and t_{ij} is the hopping integral. The effective intersite (p -wave) pairing is induced via combined effect of the Rashba and the Zeeman terms

$$\hat{\mathcal{H}}_{\text{Rashba}} = -\alpha \sum_{i,\sigma,\sigma'} \left[\hat{d}_{i+1,\sigma}^{\dagger} (i\sigma^y)_{\sigma\sigma'} \hat{d}_{i,\sigma'} + \text{H.c.} \right], \quad (11)$$

$$\hat{\mathcal{H}}_{\text{Zeeman}} = \frac{g\mu_B B}{2} \sum_{i,\sigma,\sigma'} \hat{d}_{i,\sigma}^{\dagger} (\sigma^z)_{\sigma\sigma'} \hat{d}_{i,\sigma'}. \quad (12)$$

The proximity effect, which induces the on-site (trivial) pairing, can be modelled as [45]

$$\hat{\mathcal{H}}_{\text{prox}} = \Delta_i \left(\hat{d}_{i,\uparrow}^{\dagger} \hat{d}_{i,\downarrow}^{\dagger} + \hat{d}_{i,\downarrow} \hat{d}_{i,\uparrow} \right) \quad (13)$$

with the local pairing potential $\Delta_i = \Gamma_S/2$.

Fig. 4 shows evolution of the spin-dependent spectrum $\rho_{i,\sigma}(\omega)$ with respect to varying magnetic field. At critical value ($B \simeq 0.2$) we observe emergence of the zero-energy quasiparticles, whose spectral weights strongly depend on the spin σ .

B. Spin-polarized Majorana quasiparticles

For better understanding of the polarized zero-energy quasiparticles, we present in Fig. 5 the spatial profiles of the zero-energy (Majorana) quasiparticles. As usually such quasiparticles emerge near the edges on a nanoscopic chain, practically over 10 to 15 sites (see inset). Let us notice the substantial quantitative difference between these zero-energy quasiparticles appearing in \uparrow and \downarrow spin sectors. Such ‘intrinsic polarization’ of the Majorana

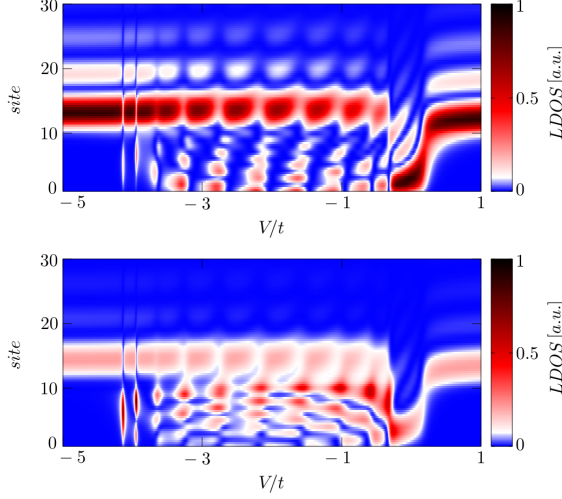


FIG. 6. Leakage of the spin-polarized Majorana quasiparticles from the topological superconducting phase of the Rashba chain ($i \geq 10$) onto the side-attached multi-site ($i \in \{1; 10\}$) quantum dot. The upper and bottom panel shows $\rho_{i,\sigma}(\omega)$ for $\omega=0$ of \uparrow and \downarrow spin, respectively.

modes has been previously suggested in Ref. [46], and recently we have proposed [47] their empirical detection by means of the Selective Equal Spin Andreev Reflection (SESAR) spectroscopy.

The main idea is to apply bias voltage V between the STM tip and the superconducting substrate, inducing the charge transport which in a subgap regime ($|V| \ll \Delta/|e|$) originates from the Andreev (particle to hole) scattering mechanism. The polarized Andreev current can be expressed by Landauer-Büttiker formula

$$I_i^\sigma(V) = \frac{e}{h} \int d\omega T_i^\sigma(\omega) [f(\omega - eV) - f(\omega + eV)], \quad (14)$$

where the transmittance $T_i^\sigma(\omega) = \Gamma_N^2 \left| \langle \hat{d}_{i\sigma} \hat{d}_{i+1\sigma} \rangle \right|^2 + \Gamma_N^2 \left| \langle \hat{d}_{i\sigma} \hat{d}_{i-1\sigma} \rangle \right|^2$ and $T_1^\sigma(\omega) = \Gamma_N^2 \left| \langle \hat{d}_{1\sigma} \hat{d}_{2\sigma} \rangle \right|^2$, $T_N^\sigma(\omega) = \Gamma_N^2 \left| \langle \hat{d}_{N\sigma} \hat{d}_{N-1\sigma} \rangle \right|^2$. The anomalous Green's functions can be computed numerically from the solution of the Bogoliubov-de Gennes equations of this model (10). The net spin current $I_i^{\text{spin}}(V) = I_i^\uparrow(V) - I_i^\downarrow(V)$ turns out to be predominantly sensitive to the Majorana end-modes. Its differential conductance $G_i^{\text{spin}}(V) = \frac{\partial}{\partial V} I_i^{\text{spin}}(V)$ can thus distinguish the polarized Majorana quasiparticle (near $V = 0$) from the YSR states (appearing at finite voltage).

C. Leakage of polarized Majorana quasiparticles

Bound states can leak to other side-attached nanoscopic objects. Such proximity effect has been also predicted for the Majorana quasiparticles by E. Vernek *et*

al. [48] and it has been indeed observed experimentally by M. T. Deng *et al.* [49]. Inspired by this achievement, there has been intensive study of the YSR states coalescing into the zero-energy Majorana state in the side-coupled quantum dots driven by electrostatic or magnetic fields [50–52]. This issue would be particularly important when attempting to braid the Majorana end modes, e.g., in T-shape nanowires upon turning on/off the topological superconducting phase in its segments. We briefly analyse here the polarized zero-energy Majorana modes leaking on the multi-site quantum dot (comprised of 10 lattice sites) side-attached to the proximitized Rashba chain (discussed above).

Fig. 6 displays spatial profile of the polarized spectrum obtained at $\omega = 0$ as function of the gate voltage V_g , which detunes the energies $V_g = \epsilon_i - \mu$ of the multi-site ($1 \leq i \leq 10$) quantum dot. For numerical calculations we used the model parameters $\lambda = 0.15t$, $\mu = -2t$, $\Delta_i = 0.2t$ and $B > B_c$, which guarantee the Rashba chain to be in its topologically nontrivial superconducting phase, hosting the zero-energy Majorana quasiparticles (intensive black or red regions). We clearly observe that for some values of V_g these Majorana modes spread over the entire quantum dot region. By inspecting Fig. 6 we furthermore notice the pronounced spatial oscillations of these zero-energy modes. In our opinion, this is a signature of a partial delocalization of the polarized Majorana quasiparticles. Surprisingly, this process seems to be less efficient in the minor spin ($\sigma = \downarrow$) section. Such effect has to be taken into account, when designing nanostructures for a controllable spatial displacement of the Majorana modes (critical for realization of quantum computations with use of the Majorana-based qubits) either by electrostatic or magnetic means. Some proposals for such nanodevices have been recently discussed by several authors [52, 53].

In summary of this section, we emphasize that the Majorana modes coalescing from the YSR states in the proximitized Rashba nanowire are characterized by their magnetic polarization. Indeed, such feature has been recently observed by STM spectroscopy with use of the polarized tip [42]. We have studied here evolution of the polarized quasiparticle states with respect to the magnetic field (Fig. 4) and investigated the spatial oscillations of the Majorana zero-energy modes near the chain edges (Fig. 5). Finally, we analyzed leakage of the polarized Majorana modes on the multi-site quantum dots, revealing their partial delocalization (Fig. 6).

IV. MAJORANA VS KONDO EFFECT

In Sec. III we have discussed the polarized Majorana modes leaking on side-attached objects, like single impurities or segments of the normal nanowires. In this section we shall focus on the correlation effects [54–56], confronting the Majorana quasiparticle with the Kondo effect (both manifested at zero energy). This can be prac-

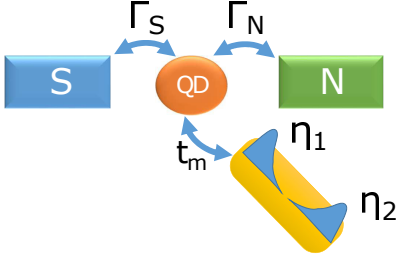


FIG. 7. Schematic illustration of the quantum dot (QD) coupled between the metallic (N) and superconducting (S) leads and hybridized with the Rashba nanowire, hosting the Majorana quasiparticles η_1 and η_2 at its edges.

tically achieved using STM-type configurations sketched in Fig. 7. In particular we consider the subgap Kondo effect, effectively driven by the Coulomb repulsion U and coupling of the quantum dot (QD) with the normal lead Γ_N in presence of the electron pairing (induced via Γ_S), which plays a prominent influence on the spin-polarized bound states of QD. Basic mechanism of this subgap Kondo effect showing up near the quantum phase transition has been earlier considered by us in absence of the Rashba nanowire [24, 57]. Our considerations can be practically verified within STM geometry [39, 40] using the magnetic atoms (e.g. Fe) and the side-coupled non-magnetic atoms (for instance Ag or Au) deposited on the superconducting substrate (like Pb or Al) and probed the conducting STM tip [42].

A. Low energy model

Topological superconducting phase, hosting the Majorana modes, can be driven in semiconducting wires [58, 59] or in nanochains of magnetic atoms [39–42] due to the nearest neighbor equal spin pairing. Efficiency of such p -wave pairing differs for each spin [47], giving rise to polarization of the Majorana quasiparticles, with noticeable preference for \uparrow sector (see Fig. 4). In order to study the correlation effects we shall assume here a complete polarization of such Majorana quasiparticles. We thus focus, for simplicity, on the topological state originating from intersite pairing of only \uparrow electrons and consider its interplay with the correlations. Let us remark, however, that superconducting lead mixes both the QD spins with the side-attached Majorana quasiparticle [60]. In consequence we shall observe an interesting and spin-dependent relationship between the Majorana and Kondo states which could be probed by the polarized Andreev (particle to hole conversion) mechanism.

Our setup (Fig. 7) can be described by the following Anderson-type Hamiltonian

$$\hat{H} = \sum_{\beta=S,N} \left(\hat{H}_\beta + \hat{H}_{\beta-QD} \right) + \hat{H}_{QD} + \hat{H}_{MQD}, \quad (15)$$

where \hat{H}_N corresponds to the metallic electrode, \hat{H}_S

refers to the s -wave superconducting substrate and the correlated QD is modeled by $\hat{H}_{QD} = \sum_\sigma \epsilon \hat{d}_\sigma^\dagger \hat{d}_\sigma + U \hat{n}_\downarrow \hat{n}_\uparrow$, where ϵ denotes the energy level and U stands for the repulsive interaction between opposite spin electrons. Such QD is coupled to both $\beta = N, S$ reservoirs via $\hat{H}_{\beta-QD} = \sum_{\mathbf{k},\sigma} (V_{\mathbf{k}\beta} \hat{d}_\sigma^\dagger \hat{c}_{\mathbf{k}\sigma\beta} + \text{H.c.})$ and we assume a wide bandwidth limit, using the constant couplings Γ_β . It can be shown [61–64] that for energies $|\omega| \ll \Delta$ the superconducting electrode induces the static on-dot pairing $\hat{H}_S + \hat{H}_{S-QD} \approx H_{\text{prox}} = \sum_\sigma \epsilon \hat{d}_\sigma^\dagger \hat{d}_\sigma + U \hat{n}_\downarrow \hat{n}_\uparrow - \frac{\Gamma_S}{2} (\hat{d}_\uparrow \hat{d}_\downarrow + \hat{d}_\downarrow^\dagger \hat{d}_\uparrow^\dagger)$. One can take into account the finite magnitude of superconducting gap [50] but this does not affect the main conclusions of our study.

The effective Majorana modes of the nanowire can be modeled by [65] $\hat{H}_{MQD} = i\epsilon_m \hat{\eta}_1 \hat{\eta}_2 + \lambda (\hat{d}_\uparrow \hat{\eta}_1 + \hat{\eta}_1 \hat{d}_\uparrow^\dagger)$, where $\hat{\eta}_i = \hat{\eta}_i^\dagger$ are hermitian operators and ϵ_m corresponds to an overlap between Majoranas. We recast these operators by the standard fermionic ones [66] $\hat{\eta}_1 = \frac{1}{\sqrt{2}}(\hat{f} + \hat{f}^\dagger)$ and $\hat{\eta}_2 = \frac{-i}{\sqrt{2}}(\hat{f} - \hat{f}^\dagger)$. Finally, the Hamiltonian (15) simplifies to

$$\begin{aligned} \hat{H} = & \hat{H}_N + \hat{H}_{N-QD} + \sum_\sigma \epsilon \hat{d}_\sigma^\dagger \hat{d}_\sigma + U \hat{n}_\downarrow \hat{n}_\uparrow - \frac{\Gamma_S}{2} (\hat{d}_\uparrow \hat{d}_\downarrow \\ & + \hat{d}_\downarrow^\dagger \hat{d}_\uparrow^\dagger) + \epsilon_m \hat{f}^\dagger \hat{f} + t_m (\hat{d}_\uparrow^\dagger - \hat{d}_\uparrow)(\hat{f} + \hat{f}^\dagger) - \frac{\epsilon_m}{2} \end{aligned} \quad (16)$$

with the auxiliary coupling $t_m = \lambda/\sqrt{2}$. The subgap Kondo physics originates in this model from the Coulomb term $U \hat{n}_\downarrow \hat{n}_\uparrow$ and the effective spin exchange interactions due to \hat{H}_{N-QD} . It has been shown [23, 24] that under specific conditions the on-dot pairing can cooperate with the subgap Kondo effect. This particular situation occurs only near the quantum phase transition.

B. Spin-dependent spectrum

Let us examine how the subgap Kondo effect gets along with the Majorana mode. Earlier studies of the correlated quantum dot coupled to both normal (conducting) electrodes indicated that the side-attached Rashba chain leads to competition between the Kondo and Majorana states [67–72]. For sufficiently long wire ($\epsilon_m = 0$) the Kondo effect survives only in the spin-channel \downarrow , whereas for \uparrow electrons there appears a dip in the spectral density at $\omega = 0$. The resulting tunneling conductance is then partly reduced (from the perfect value $2e^2/h$) to the fractional value $3e^2/2h$ [67, 68, 71–73]. On contrary, for the short Rashba wires (with $\epsilon_m \neq 0$) the Kondo physics survives in both spin channels.

In our present setup (Fig. 7) the correlated quantum dot is between the metallic and superconducting reservoirs, therefore the Kondo effect is additionally affected by the on-dot pairing. Its influence is mainly controlled by the ratio U/Γ_S and partly by the level ϵ , deciding whether the QD ground-state is in the spinful or spinless configuration [23, 24, 62, 64, 74]. Obviously the latter

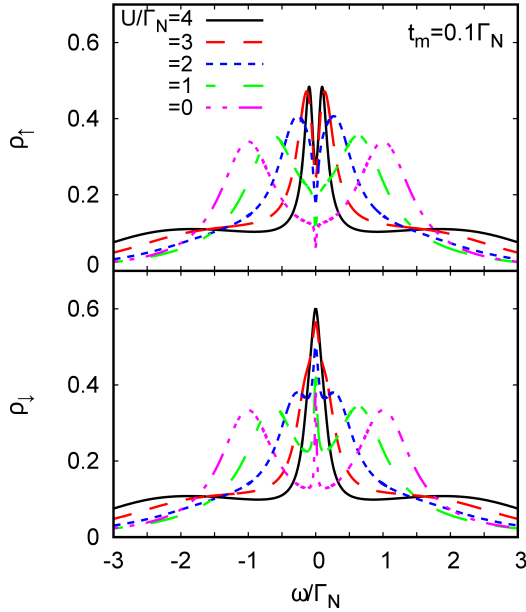


FIG. 8. The polarized spectral function $\rho_\sigma(\omega)$ obtained at zero temperature for the half-filled QD ($\varepsilon = -U/2$), $\Gamma_S = 2\Gamma_N$, $t_m = 0.1\Gamma_N$ and several values of the Coulomb potential U (as indicated). Energies are expressed in units of Γ_N .

one cannot be screened. For instance, for the half-filled QD ($\varepsilon = -U/2$) the spinful (doublet) configuration occurs in the regime $U \geq \Gamma_S$.

For studying the correlations we adopt perturbative treatment of the Coulomb potential, treating it self-consistently to the second order in the normal and anomalous channels [62, 75]. Specific expressions have been given by us in Ref. [24]. Fig. 8 shows the spectral function $\rho_\sigma(\omega)$ for both spins obtained at zero temperature for the Coulomb potential U , covering the (spinless) singlet and (spinful) doublet configurations. In the weak interaction regime we observe appearance of two YSR states. For $U \approx \Gamma_S$ these peaks merge, signaling the quantum phase transition. The Kondo effect shows up only in the correlated limit ($U > \Gamma_S$), but its spectroscopic signatures are qualitatively different for each of the spins. Leakage of the Majorana quasiparticle suppresses the low energy states of \uparrow electrons. We notice that the initial density (for $t_m = 0$) is reduced by half, whereas we observe a constructive influence of the Majorana quasiparticle on opposite spin \downarrow electrons.

Fig. 9 shows evolution of the spectral function $\rho_\uparrow(\omega)$ for various couplings t_m . In the weak coupling limit we clearly observe reduction (by half) of the initial density of states. With increasing t_m the spectrum develops the three-peak structure, typical for the 'molecular' limit. Such behavior indicates that the Majorana and Kondo states have rather a complicated relation, which is neither competitive nor cooperative. In fact, some novel scaling laws have been recently reported by several authors [69, 70, 76–79] although considering the correlation

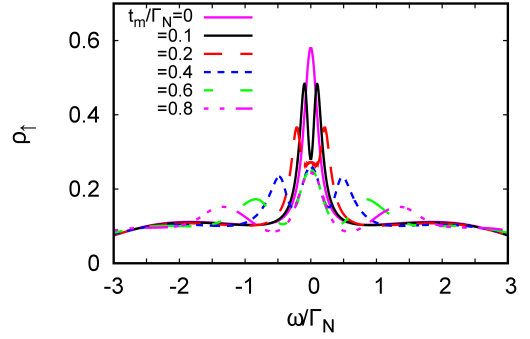


FIG. 9. The spectral function $\rho_\uparrow(\omega)$ of the half-filled quantum dot ($\varepsilon = -U/2$) obtained at $T = 0$ for $\Gamma_S/\Gamma_N = 2$, $U/\Gamma_N = 4$ and several values of t_m (as indicated).

effects directly in the Rashba nanowire.

V. CONCLUSIONS

We have studied the polarized bound states of magnetic impurities embedded in the s -wave superconducting material, taking into account the spin-orbit and/or Coulomb interactions. We have shown that SO coupling strongly affects the subgap states, both of the single impurities and their conglomerates arranged into nanoscopic chain. For the case of single magnetic impurity the SO interaction (i) shifts the quantum phase transition towards higher magnetic coupling J_c , (ii) enhances spatial size of the YSR states, and (iii) smoothens the particle-hole oscillations. For the magnetic chain such SO coupling combined with the Zeeman term induce the topologically nontrivial superconducting state and indirectly give rise to substantial polarization of the Majorana modes (Fig. 4), whose oscillations show up near the chain edges (Fig. 5). The polarized Majorana quasiparticles can also leak onto other side-coupled objects, like the single or multiple quantum impurities (Fig. 6). These polarized Majorana quasiparticles can be controlled by the magnetic field or by electrostatic potential (that would be important for future quantum computations using the qubits based on topologically protected Majorana states). Finally, we have also confronted the Majorana quasiparticles with the subgap Kondo effect, revealing their complex relationship which can be hardly regarded as competitive or collaborative in some analogy to the Kondo effect originating from multiple degrees of freedom [80]. The aforementioned spin-polarized effects can be experimentally verified by the polarized ballistic tunneling or using STM spectroscopy, relying on the selective equal spin Andreev reflections.

ACKNOWLEDGMENTS

We thank for instructive remarks from R. Aguado, J. Klinovaja, R. Lutchyn, P. Simon, and R. Žitko on different parts of our study. This work was supported by the National Science Centre (Poland)

under grants DEC-2014/13/B/ST3/04451 (AK, SG, TD) and DEC-2013/11/B/ST3/00824 (MMM) UMO-2017/25/B/ST3/02586 (AP) and by the Faculty of Mathematics and Natural Sciences of the University of Rzeszów through the project WMP/GD-06/2017 (GG).

-
- [1] S. Choi, H. J. Choi, J. M. Ok, Y. Lee, W.-J. Jang, A. T. Lee, Y. Kuk, S.B. Lee, A. J. Heinrich, S.-W. Cheong, Y. Bang, S. Johnston, J. S. Kim, and J. Lee, “Switching magnetism and superconductivity with spin-polarized current in iron-based superconductor,” *Phys. Rev. Lett.* **119**, 227001 (2017).
 - [2] M. Kenzelmann, Th. Strässle, C. Niedermayer, M. Sigrist, B. Padmanabhan, M. Zolliker, A. D. Bianchi, R. Movshovich, E. D. Bauer, J. L. Sarrao, and J. D. Thompson, “Coupled superconducting and magnetic order in CeCoIn_5 ,” *Science* **321**, 1652 (2008).
 - [3] H. W. Meul, C. Rossel, M. Decroux, Ø Fischer, G. Remenyi, and A. Briggs, “Observation of magnetic-field-induced superconductivity,” *Phys. Rev. Lett.* **53**, 497 (1984).
 - [4] A. V. Balatsky, I. Vekhter, and J.-X. Zhu, “Impurity-induced states in conventional and unconventional superconductors,” *Rev. Mod. Phys.* **78**, 373 (2006).
 - [5] B. W. Heinrich, J. I. Pascual, and K. J. Franke, “Single magnetic adsorbates on s-wave superconductors,” arXiv:1705.03672 (2017).
 - [6] A. Yazdani, B. A. Jones, C. P. Lutz, M. F. Crommie, and D. M. Eigler, “Probing the local effects of magnetic impurities on superconductivity,” *Science* **275**, 1767 (1997).
 - [7] S.-H. Ji, T. Zhang, Y.-S. Fu, X. Chen, X.-C. Ma, J. Li, W.-H. Duan, J.-F. Jia, and Q.-K. Xue, “High-resolution scanning tunneling spectroscopy of magnetic impurity induced bound states in the superconducting gap of Pb thin films,” *Phys. Rev. Lett.* **100**, 226801 (2008).
 - [8] K. J. Franke, G. Schulze, and J. I. Pascual, “Competition of superconducting phenomena and Kondo screening at the nanoscale,” *Science* **332**, 940 (2011).
 - [9] M. Ruby, F. Pientka, Y. Peng, F. von Oppen, B. W. Heinrich, and K. J. Franke, “Tunneling processes into localized subgap states in superconductors,” *Phys. Rev. Lett.* **115**, 087001 (2015).
 - [10] N. Hatter, B. W. Heinrich, M. Ruby, J. I. Pascual, and K. J. Franke, “Magnetic anisotropy in Shiba bound states across a quantum phase transition,” *Nat. Commun.* **6**, 8988 (2015).
 - [11] G. C. Ménard, S. Guissart, C. Brun, S. Pons, V. S. Stolyarov, F. Debontridder, M. V. Leclerc, E. Janod, L. Cario, D. Roditchev, P. Simon, and T. Cren, “Coherent long-range magnetic bound states in a superconductor,” *Nat. Phys.* **11**, 1013 (2015).
 - [12] A. Jellinggaard, K. Grove-Rasmussen, M. H. Madsen, and J. Nygård, “Tuning Yu-Shiba-Rusinov states in a quantum dot,” *Phys. Rev. B* **94**, 064520 (2016).
 - [13] D.-J. Choi, C. Rubio-Verdú, J. de Bruijkere, M. M. Ugeda, N. Lorente, and J. I. Pascual, “Mapping the orbital structure of impurity bound states in a superconductor,” *Nat. Commun.* **8**, 15175 (2017).
 - [14] A. Assouline, Ch. Feuillet-Palma, A. Zimmers, M. Aubin, H. Aprili, and J.-Ch. Harmand, “Shiba bound states across the mobility edge in doped InAs nanowires,” *Phys. Rev. Lett.* **119**, 097701 (2017).
 - [15] M. I. Salkola, A. V. Balatsky, and J. R. Schrieffer, “Spectral properties of quasiparticle excitations induced by magnetic moments in superconductors,” *Phys. Rev. B* **55**, 12648 (1997).
 - [16] M. E. Flatté and J. M. Byers, “Local electronic structure of a single magnetic impurity in a superconductor,” *Phys. Rev. Lett.* **78**, 3761 (1997).
 - [17] M. M. Ugeda, A. J. Bradley, Y. Zhang, S. Onishi, Y. Chen, W. Ruan, C. Ojeda-Aristizabal, H. Ryu, M. T. Edmonds, H.-Z. Tsai, A. Riss, S.-K. Mo, D. Lee, A. Zettl, Z. Hussain, Z.-X. Shen, and M. F. Crommie, “Characterization of collective ground states in single-layer NbSe_2 ,” *Nat. Phys.* **12**, 92 (2016).
 - [18] S. Kezilebieke, M. Dvorak, T. Ojanen, and P. Liljeroth, “Coupled Yu-Shiba-Rusinov states in molecular dimers on NbSe_2 ,” arXiv:1701.03288 (2017).
 - [19] H. Santos, David Soriano, and J. J. Palacios, “Anomalous exchange interaction between intrinsic spins in conducting graphene systems,” *Phys. Rev. B* **89**, 195416 (2014).
 - [20] Y. Kim, J. Zhang, E. Rossi, and R. M. Lutchyn, “Impurity-induced bound states in superconductors with spin-orbit coupling,” *Phys. Rev. Lett.* **114**, 236804 (2015).
 - [21] V. Kaladzhyan, C. Bena, and P. Simon, “Characterizing p -wave superconductivity using the spin structure of Shiba states,” *Phys. Rev. B* **93**, 214514 (2016).
 - [22] A. Ptok, S. Głodzik, and T. Domański, “Yu-Shiba-Rusinov states of impurities in a triangular lattice of NbSe_2 with spin-orbit coupling,” *Phys. Rev. B* **96**, 184425 (2017).
 - [23] R. Žitko, J. Soo Lim, R. López, and R. Aguado, “Shiba states and zero-bias anomalies in the hybrid normal-superconductor Anderson model,” *Phys. Rev. B* **91**, 045441 (2015).
 - [24] T. Domański, I. Weymann, M. Barańska, and G. Górski, “Constructive influence of the induced electron pairing on the Kondo state,” *Sci. Rep.* **6**, 23336 (2016).
 - [25] E. D. B. Smith, K. Tanaka, and Y. Nagai, “Manifestation of chirality in the vortex lattice in a two-dimensional topological superconductor,” *Phys. Rev. B* **94**, 064515 (2016).
 - [26] S. L. Goertzen, K. Tanaka, and Y. Nagai, “Self-consistent study of Abelian and non-Abelian order in a two-dimensional topological superconductor,” *Phys. Rev. B* **95**, 064509 (2017).
 - [27] V. Koerting, B. M. Andersen, K. Flensberg, and J. Paaske, “Nonequilibrium transport via spin-induced subgap states in superconductor/quantum dot/normal

- metal cotunnel junctions,” *Phys. Rev. B* **82**, 245108 (2010).
- [28] S. S. Pershoguba, K. Björnson, A. M. Black-Schaffer, and A. V. Balatsky, “Currents induced by magnetic impurities in superconductors with spin-orbit coupling,” *Phys. Rev. Lett.* **115**, 116602 (2015).
- [29] Sz. Głodzik and A. Ptok, “Quantum phase transition induced by magnetic impurity,” *J. Supercond. Nov. Magn.* (2017), 10.1007/s10948-017-4360-6.
- [30] M. Mashkooi, K. Björnson, and A. M. Black-Schaffer, “Impurity bound states in fully gapped d-wave superconductors with subdominant order parameters,” *Sci. Rep.* **7**, 44107 (2017).
- [31] K. Satori, H. Shiba, O. Sakai, and Y. Shimizu, “Numerical Renormalization Group study of magnetic impurities in superconductors,” *Journal of the Physical Society of Japan* **61**, 3239–3254 (1992), <https://doi.org/10.1143/JPSJ.61.3239>.
- [32] O. Sakai, Y. Shimizu, H. Shiba, and K. Satori, “Numerical Renormalization Group study of magnetic impurities in superconductors. II. Dynamical excitation spectra and spatial variation of the order parameter,” *Journal of the Physical Society of Japan* **62**, 3181–3197 (1993), <https://doi.org/10.1143/JPSJ.62.3181>.
- [33] A. Sakurai, “Comments on superconductors with magnetic impurities,” *Prog. Theor. Phys.* **44**, 1472 (1970).
- [34] W.-V. van Gerven Oei, D. Tanasković, and R. Žitko, “Magnetic impurities in spin-split superconductors,” *Phys. Rev. B* **95**, 085115 (2017).
- [35] D. K. Morr and J. Yoon, “Impurities, quantum interference, and quantum phase transitions in s-wave superconductors,” *Phys. Rev. B* **73**, 224511 (2006).
- [36] J. Röntynen and T. Ojanen, “Topological superconductivity and high Chern numbers in 2D ferromagnetic Shiba lattices,” *Phys. Rev. Lett.* **114**, 236803 (2015).
- [37] D. K. Morr and N. A. Stavropoulos, “Quantum interference between impurities: Creating novel many-body states in s-wave superconductors,” *Phys. Rev. B* **67**, 020502 (2003).
- [38] T. Kawakami and X. Hu, “Evolution of density of states and a spin-resolved checkerboard-type pattern associated with the majorana bound state,” *Phys. Rev. Lett.* **115**, 177001 (2015).
- [39] S. Nadj-Perge, I. K. Drozdov, J. Li, H. Chen, S. Jeon, J. Seo, A. H. MacDonald, B. A. Bernevig, and A. Yazdani, “Observation of Majorana fermions in ferromagnetic atomic chains on a superconductor,” *Science* **346**, 602 (2014).
- [40] R. Pawlak, M. Kisiel, J. Klinovaja, T. Maier, S. Kawai, T. Glatzel, D. Loss, and E. Meyer, “Probing atomic structure and Majorana wave-functions in mono-atomic Fe-chains on superconducting Pb-surface,” *npj Quantum Info* **2**, 16035 (2016).
- [41] M. Ruby, F. Pientka, Y. Peng, F. von Oppen, B. W. Heinrich, and K. J. Franke, “End states and subgap structure in proximity-coupled chains of magnetic adatoms,” *Phys. Rev. Lett.* **115**, 197204 (2015).
- [42] S. Jeon, Y. Xie, J. Li, Z. Wang, B. A. Bernevig, and A. Yazdani, “Distinguishing a Majorana zero mode using spin-resolved measurements,” *Science* **358**, 772 (2017).
- [43] M. M. Maška, A. Gorczyca-Goraj, J. Tworzydło, and T. Domański, “Majorana quasiparticles of an inhomogeneous Rashba chain,” *Phys. Rev. B* **95**, 045429 (2017).
- [44] X. Liu, X. Li, D.-L. Deng, X.-J. Liu, and S. Das Sarma, “Majorana spintronics,” *Phys. Rev. B* **94**, 014511 (2016).
- [45] T. D. Stanescu and S. Tewari, “Majorana fermions in semiconductor nanowires: fundamentals, modeling, and experiment,” *J. Phys.: Condens. Matter* **25**, 233201 (2013).
- [46] D. Sticlet, C. Bena, and P. Simon, “Spin and Majorana polarization in topological superconducting wires,” *Phys. Rev. Lett.* **108**, 096802 (2012).
- [47] M. M. Maška and T. Domański, “Polarization of the majorana quasiparticles in the Rashba chain,” *Sci. Rep.* **7**, 16193 (2017).
- [48] E. Vernek, P. H. Penteado, A. C. Seridonio, and J. C. Egues, “Subtle leakage of a Majorana mode into a quantum dot,” *Phys. Rev. B* **89**, 165314 (2014).
- [49] M. T. Deng, S. Vaitiekėnas, E. B. Hansen, J. Danon, M. Leijnse, K. Flensberg, J. Nygård, P. Krogstrup, and C. M. Marcus, “Majorana bound state in a coupled quantum-dot hybrid-nanowire system,” *Science* **354**, 1557 (2016).
- [50] C.-X. Liu, J. D. Sau, T. D. Stanescu, and S. Das Sarma, “Andreev bound states versus Majorana bound states in quantum dot-nanowire-superconductor hybrid structures: Trivial versus topological zero-bias conductance peaks,” *Phys. Rev. B* **96**, 075161 (2017).
- [51] S. Hoffman, D. Chevallier, D. Loss, and J. Klinovaja, “Spin-dependent coupling between quantum dots and topological quantum wires,” *Phys. Rev. B* **96**, 045440 (2017).
- [52] A. Ptok, A. Kobińska, and T. Domański, “Controlling the bound states in a quantum-dot hybrid nanowire,” *Phys. Rev. B* **96**, 195430 (2017).
- [53] D. Chevallier, P. Szumniak, S. Hoffman, D. Loss, and J. Klinovaja, “Topological phase detection in Rashba nanowires with a quantum dot,” arXiv:1710.05576 (2017).
- [54] R. Chirla and C. P. Moca, “Fingerprints of Majorana fermions in spin-resolved subgap spectroscopy,” *Phys. Rev. B* **94**, 045405 (2016).
- [55] E. Prada, R. Aguado, and P. San-Jose, “Measuring Majorana nonlocality and spin structure with a quantum dot,” *Phys. Rev. B* **96**, 085418 (2017).
- [56] J. Barański, A. Kobińska, and T. Domański, “Spin-sensitive interference due to Majorana state on the interface between normal and superconducting leads,” *J. Phys.: Condens. Matter* **29**, 075603 (2017).
- [57] T. Domański, M. Žonda, V. Pokorný, G. Górski, V. Janiš, and T. Novotný, “Josephson-phase-controlled interplay between correlation effects and electron pairing in a three-terminal nanostructure,” *Phys. Rev. B* **95**, 045104 (2017).
- [58] V. Mourik, K. Zuo, S. M. Frolov, S. R. Plissard, E. P. A. M. Bakkers, and L. P. Kouwenhoven, “Signatures of Majorana fermions in hybrid superconductor-semiconductor nanowire devices,” *Science* **336**, 1003 (2012).
- [59] Hao Zhang, Önder Gül, Sonia Conesa-Boj, Kun Zuo, Vincent Mourik, Folkert K. de Vries, Jasper van Veen, David J. van Woerkom, Michał P. Nowak, Michael Wimmer, Diana Car, Sbastien Plissard, Erik P. A. M. Bakkers, Marina Quintero-Pérez, Srijit Goswami, Kenji Watanabe, Takashi Taniguchi, and Leo P. Kouwenhoven, “Ballistic Majorana nanowire devices,” arXiv:1603.04069

- (2016).
- [60] A. Golub, “Multiple Andreev reflections in s -wave superconductor-quantum dot-topological superconductor tunnel junctions and Majorana bound states,” *Phys. Rev. B* **91**, 205105 (2015).
 - [61] J. Bauer, A. Oguri, and A. C. Hewson, “Spectral properties of locally correlated electrons in a Bardeen-Cooper-Schrieffer superconductor,” *J. Phys.: Condens. Matter* **19**, 486211 (2007).
 - [62] Y. Yamada, Y. Tanaka, and N. Kawakami, “Interplay of Kondo and superconducting correlations in the nonequilibrium Andreev transport through a quantum dot,” *Phys. Rev. B* **84**, 075484 (2011).
 - [63] A. Martín-Rodero and A. Levy Yeyati, “Josephson and Andreev transport through quantum dots,” *Advances in Physics* **60**, 899 (2011).
 - [64] J. Barański and T. Domański, “In-gap states of a quantum dot coupled between a normal and a superconducting lead,” *J. Phys.: Condens. Matter* **25**, 435305 (2013).
 - [65] D. E. Liu, M. Cheng, and R. M. Lutchyn, “Probing Majorana physics in quantum-dot shot-noise experiments,” *Phys. Rev. B* **91**, 081405 (2015).
 - [66] S. R. Elliott and M. Franz, “Colloquium: Majorana fermions in nuclear, particle, and solid-state physics,” *Rev. Mod. Phys.* **87**, 137 (2015).
 - [67] D. A. Ruiz-Tijerina, E. Vernek, L. G. G. V. Dias da Silva, and J. C. Egues, “Interaction effects on a Majorana zero mode leaking into a quantum dot,” *Phys. Rev. B* **91**, 115435 (2015).
 - [68] M. Lee, J. S. Lim, and R. López, “Kondo effect in a quantum dot side-coupled to a topological superconductor,” *Phys. Rev. B* **87**, 241402 (2013).
 - [69] M. Cheng, M. Becker, B. Bauer, and R. M. Lutchyn, “Interplay between Kondo and Majorana interactions in quantum dots,” *Phys. Rev. X* **4**, 031051 (2014).
 - [70] I. J. van Beek and B. Braunecker, “Non-Kondo many-body physics in a Majorana-based Kondo type system,” *Phys. Rev. B* **94**, 115416 (2016).
 - [71] I. Weymann, “Spin Seebeck effect in quantum dot side-coupled to topological superconductor,” *J. Phys.: Condens. Matter* **29**, 095301 (2017).
 - [72] I. Weymann and K. P. Wójcik, “Transport properties of a hybrid Majorana wire-quantum dot system with ferromagnetic contacts,” *Phys. Rev. B* **95**, 155427 (2017).
 - [73] R. López, M. Lee, L. Serra, and J. S. Lim, “Thermoelectrical detection of Majorana states,” *Phys. Rev. B* **89**, 205418 (2014).
 - [74] Y. Tanaka, N. Kawakami, and A. Oguri, “Numerical renormalization group approach to a quantum dot coupled to normal and superconducting leads,” *J. Phys. Soc. Japan* **76**, 074701 (2007).
 - [75] E. Vecino, A. Martín-Rodero, and A. Levy Yeyati, “Josephson current through a correlated quantum level: Andreev states and π junction behavior,” *Phys. Rev. B* **68**, 035105 (2003).
 - [76] B. Béri and N. R. Cooper, “Topological kondo effect with majorana fermions,” *Phys. Rev. Lett.* **109**, 156803 (2012).
 - [77] M. R. Galpin, A. K. Mitchell, J. Temaismithi, D. E. Logan, B. Béri, and N. R. Cooper, “Conductance fingerprint of majorana fermions in the topological kondo effect,” *Phys. Rev. B* **89**, 045143 (2014).
 - [78] S. Plugge, A. Zazunov, E. Eriksson, A. M. Tsvelik, and R. Egger, “Kondo physics from quasiparticle poisoning in majorana devices,” *Phys. Rev. B* **93**, 104524 (2016).
 - [79] B. Béri, “Exact nonequilibrium transport in the topological kondo effect,” *Phys. Rev. Lett.* **119**, 027701 (2017).
 - [80] D. Jacob, M. Soriano, and J. J. Palacios, “Kondo effect and spin quenching in high-spin molecules on metal substrates,” *Phys. Rev. B* **88**, 134417 (2013).